Freehand 3D Ultrasound Calibration Using an Electromagnetically Tracked Needle

Hui Zhang[a], Filip Banovac[a,b], Amy White[b], Kevin Cleary[a*]
[a]Imaging Science and Information Systems (ISIS) Center,
Department of Radiology, Georgetown University Medical Center
2115 Wisconsin Ave. NW, Suite 603, Washington, DC, 20007, USA
[b]Department of Radiology, Georgetown University Hospital
3800 Reservoir Road, Washington, DC, 20007, USA

ABSTRACT

Freehand 3D ultrasound allows intra-operative imaging of volumes of interest in a fast and flexible way. However, the ultrasound device must be calibrated before it can be registered with other imaging modalities. We present a needle-fiducial based electromagnetic localization approach for calibrating freehand 3D ultrasound as a prerequisite for creating an intra-operative navigation system. Although most existing calibration methods require a complex and tedious experiment using a customized calibration phantom, our method does not. The calibration set-up requires only a container of water and only several frames (three to nine) to detect an electromagnetically tracked needle tip in a 2D ultrasound image. The tracked needle is dipped into the water and moved freehand to locate the tip in the ultrasound imaging plane. The images that show the needle tip are recorded and the coordinates are manually or automatically identified. For each frame, the pixel indices, as well as the discrete coordinates of the tracker and the needle, are used as the inputs, and the calibration matrix is reconstructed. Three group positions, each with nine frames, are recorded for calibration and validation. Despite the lower accuracy of the electromagnetic tracking device compared to optical tracking devices, the maximum RMS error for calibration is 1.22mm with six or more frames, which shows that our proposed approach is accurate and feasible.

Keywords: freehand 3D ultrasound, ultrasound calibration, electromagnetic tracking

1. INTRODUCTION

Three-dimensional freehand ultrasound has great promise for many surgical applications, especially in minimally invasive procedures. Potential applications include 3D anatomic visualization of pathologic tissue and various ultrasound-guided procedures. Freehand tracked ultrasound can been used to create images for organ volume measurements. We are currently developing a surgical navigation system for abdominal procedures based on the electromagnetic tracking device. We have successfully completed several phantom and pig studies, but the system has yet to incorporate real-time validation of anatomical locations and respiration deformation. For this reason, we introduced a 3D freehand ultrasound device into our navigation system. The advantages of the ultrasound-based system are that it provides real-time images and can be easily integrated into the operating room.

A requirement for 3D freehand ultrasound imaging is a motion tracking system that monitors the position and orientation of a tracked transducer. Other investigators have created 3D freehand ultrasound with tracking systems that utilize electromagnetic sensors, optical sensors, acoustic speak gaps, or a combination of these types [1-8]. The advantage of a 3D freehand tracked ultrasound system over a standard, commercial ultrasound machine with 3D image reconstruction capabilities is the ability to acquire ultrasound images in a universal coordinate frame, to which other tracked surgical instruments can be attached. In addition, the movement of the tracked probe is not restricted by a small range or limited direction. By tracking the device in a common coordinate system with the patient, the surgeon can be provided with 3D information registered to the patient anatomy.

The first step required to integrate ultrasound into these systems is a calibration step as presented in this paper.

* cleary@georgetown.edu; Telephone 1-202-687-8253; Fax 1-202-784-3479

In ultrasound image calibration, the 3D physical dimensions of the beam plane are computed with respect to the tracked device. After the calibration process is completed, standard 2D B-mode ultrasound images can be reconstructed into a 3D volume using the positional information obtained from the tracking system.

There are four general methods to construct an ultrasound volume: 1. constrained sweeping techniques; 2. 3D probes; 3. sensorless techniques; and 4. 2D tracked probe (freehand) techniques [9]. Calibration must be performed to determine the position of the ultrasound coordinate system in relation to the reference coordinates of the tracking system. This calibration is most often performed by registration between the ultrasound image and a geometrical model of the phantom reconstructed from a CT image, or by touching a pre-calibrated pointer. These methods are referred to as point-based calibration methods, and are implemented by matching corresponding points from two different coordinate frames. The high accuracy of point-based calibration methods has been demonstrated by several research groups [1,10]. These techniques carry the advantage of having a simple experiment set-up, but can be more time consuming than other automated techniques, such as surface- and intensity-based mappings, because the identification of the points in the images is a manual process.

The results of several ultrasound beam calibration techniques indicate that the point-based "cross-wire" phantom produced the most precise and accurate reconstructions. Overall, an optical tracking system will provide a better calibration results than electromagnetic systems since optical systems are more accurate and not subject to disturbance from metal objects. In the "cross-wire" phantom study, a RMS of 1.65mm was obtained using an optical tracking system, while an RMS error of 2.41mm was obtained using an electromagnetic tracking system [11]. Instead of using specific calibration phantoms, we use a tracked needle as the indicator to avoid the registration and touching steps that can introduce unnecessary calibration errors. Several researchers have experimented with different approaches using point objects (such as a pinhead or a small suspended head) instead of the cross-wire phantom. For example, Muratore and Galloway used the tip of an optically tracked pointer to find the spatial transformation [12]. We use an electromagnetically tracked needle, and take a different mathematical approach to calculate the calibration matrix.

2. MATERIALS AND METHODS

2.1. Tracked ultrasound image acquisition

The ultrasound device used in the experiment is a portable system from Terason Inc. (Burlington, MA). It has 128 channels and connects with the computer through a standard IEEE 1394 firewire port. The electromagnetic tracking device is the AURORA from Northern Digital Inc. (Ontario, Canada). The digital ultrasound image is acquired from the firewire connection directly. We have found the tracking accuracy of this system to be minimally affected by small metal instruments in close proximity. The tracker attached to the ultrasound probe must be a six degree of freedom (DOF) tracker, which includes translation and rotation. The general set-up is shown in Figure 1. The tracked ultrasound probe is fixed by a plastic holder, and the bean surface contacts the water. The tracked needle is placed in a plastic cube in the water, which stabilizes the needle and can reduce the error generated by small unintentional hand movements.

The acquired ultrasound image is shown in Figure 2. The bright line at the bottom of the image is the water container. Because the entire experiment is set-up in a container of water, the contrast allows adequate visualization of the needle, and the needle tip can therefore be easily identified manually. On ultrasound the needle tip is not sharply demarcated, but is located at the center of the bright signal observed on imaging as shown in Figure 2.

2.2. Pivot calibration of electromagnetic tracker

Before performing the calibration, we pivoted the needle to get the correct offset from the tracked sensor position to the tip [13]. By applying the calibration transforms into the tracking information, the registration step of physical and tracking space, discussed previously in the point-based calibration methods, will be avoided. The position and orientation information reported by the AURORA tracking system is the center position of the sensor coil. When the sensor coil is embedded in a surgical tool, the transformation between the coil and the tip of the tool is required. This information is typically determined by a pivot calibration, in which the tip of the instrument is placed in a small hole (divot) and the instrument is rotated back and forth as sensor data is collected.

Figure 1: Experimental set-up (electromagnetic field generator, tracked ultrasound probe, needle in plastic block, water container)

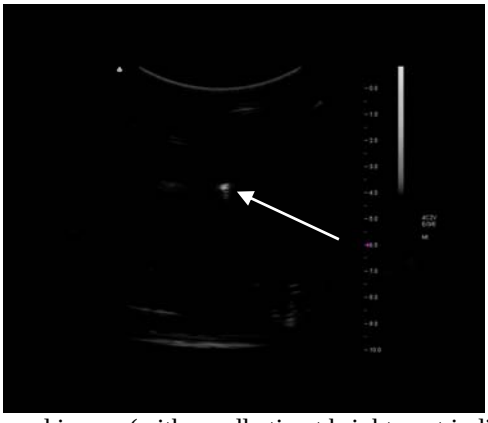

Figure 2: Ultrasound image (with needle tip at bright spot indicated by arrow)

The AURORA system returns the translational position of the sensor coil relative to a coordinate system fixed at the center of the field generator. The orientation of the sensor is also returned and specified using quaternions. Typical AURORA sensors are five degree of freedom sensors in that they cannot resolve their orientation about their long axis (the roll axis). The tracked needle used in this experiment is 5DOF. From the translational and orientation information, a four by four homogenous transformation matrix can be constructed. When the sensor coil is embedded into the needle, the long axis of the coil is parallel to the needle such that the only offset from the coil to the needle tip is along the z-axis of the needle. The transformation from the field generator coordinate system to the needle tip coordinate system can then be calculated from:

$$\begin{bmatrix} r_{00} & r_{01} & r_{02} & t_x \\ r_{10} & r_{11} & r_{12} & t_y \\ r_{20} & r_{21} & r_{22} & t_z \\ 0 & 0 & 0 & 1 \end{bmatrix} \begin{bmatrix} 0 \\ 0 \\ offset \\ 1 \end{bmatrix} = \begin{bmatrix} x_0 \\ y_0 \\ z_0 \\ 1 \end{bmatrix} \quad (1)$$

In this equation, R is the rotation matrix, T is the translation vector and (x_0, y_0, z_0) is the pivot position (in this case the tip of the needle).

Typically, we record several hundred samples while pivoting the needle. Equation (1) can be re-written as follows where the unknown variables of offset and (x_0, y_0, z_0) can be seen:

$$\begin{aligned} r_{02} \cdot offset - 1 \cdot x_0 + 0 \cdot y_0 + 0 \cdot z_0 &= -t_x \\ r_{12} \cdot offset + 0 \cdot x_0 - 1 \cdot y_0 + 0 \cdot z_0 &= -t_y \\ r_{22} \cdot offset + 0 \cdot x_0 + 0 \cdot y_0 - 1 \cdot z_0 &= -t_z \end{aligned} \tag{2}$$

These equations can then be written as:

$$A * offset + B * x_0 + C * y_0 + D * z_0 = E \tag{3}$$

In equation (3), A, B, C, D and E are the column coefficient vectors, which can then be re-written as:

$$M \cdot \begin{bmatrix} offset \\ x_0 \\ y_0 \\ z_0 \end{bmatrix} = N \tag{4}$$

Since M is not a square matrix, the unknowns can be found using the singular value decomposition (SVD) or Moore-Penrose inverse:

$$\begin{bmatrix} offset \\ x_0 \\ y_0 \\ z_0 \end{bmatrix} = \left(M^T \cdot M\right)^{-1} \cdot M^T \cdot N \tag{5}$$

Additionally, the RMS error can be computed as:

$$rms = \sqrt{\left| M \cdot \begin{bmatrix} offset & x_0 & y_0 & z_0 \end{bmatrix}^T - N \right|^2 / num} \tag{6}$$

where *num* is the number of samples.

2.3. Calibration of the ultrasound probe

To set up the experiment, we placed the ultrasound probe into a container of water. After the probe and the field generator were fixed at several different positions, the tracked needle was dipped into the water and moved to determine the exact position where the tip intersected with the imaging plane. The transformation relationship of the calibration system is shown in Figure 3.

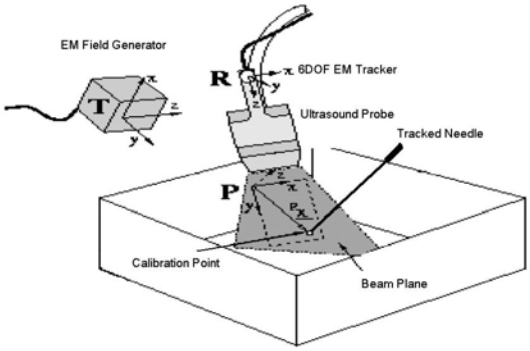

Figure 3: Calibration coordinates system, adapted from [5]

The position of the needle tip, $P_{tip,}$ can be determined by its pixel location in the ultrasound image, P_{us}, the calibration matrix, T_c, and the reference tracker's transformation matrix, T_{ref}, using the following equation:

$$P_{tip} = T_{ref} \cdot T_c \cdot P_{us} \tag{7}$$

where $P_{us} = (u, v, 0, 1)^T$, and u and v are the column and row indices of the pixel in the acquired image. The index along the z-axis is set to 0 because we used a 2D beam. The scale factors are integrated with the calibration matrix, T_c, such that the extra scale factor in the computation is not required. After left multiplying the inverse of the reference transformation matrix T_{ref}, equation (7) can be written as:

$$P_{tip/ref} = T_{ref}^{-1} \cdot P_{tip} = T_c \cdot P_{us} = T_c \cdot (u, v, 0, 1)^T \tag{8}$$

where $P_{tip/ref}$ is a vector. After taking n frames, equation (8) is accumulated as:

$$\left(P_{tip/ref,1}, \cdots P_{tip/ref,n}\right) = T_c \cdot \begin{pmatrix} u_1 & & u_n \\ v_1 & \cdots & v_n \\ 0 & & 0 \\ 1 & & 1 \end{pmatrix} = T_c \cdot T_{us} \tag{9}$$

where $T_{us} = \begin{pmatrix} u_1 & & u_n \\ v_1 & \cdots & v_n \\ 0 & & 0 \\ 1 & & 1 \end{pmatrix}$. The calibration matrix is calculated by SVD solution using

$$T_c = \left(P_{tip/ref,1}, \cdots P_{tip/ref,n}\right) \cdot T_{us}^T \cdot \left(T_{us} \cdot T_{us}^T\right)^{-1} \tag{10}$$

This computation results in a matrix with a zero vector in the third column, for the T_{us} contains a zero vector and a 1 vector in the third and forth rows. The non-zero full matrix is computed with Horn's method [14].

2.4. Algorithm validation

The validation of the calibration is significant since it confirms that the calibration matrix computed will accurately reconstruct the 3D plane in the tracking space. There are four general methods to validate the calibration matrix: the first is to calculate the RMS of the solution; the second is to use some other points which are not included in calibration computation to verify the transformation accuracy; the third is to measure the orthgonality and normality conditions of the rotation matrix of the calibration term; and the fourth is to compare the resliced image with the acquired ultrasound image plane directly.

The general transformation matrix by the rotation and translation is

$$T = \begin{bmatrix} r_{11} & r_{12} & r_{13} & t_x \\ r_{21} & r_{22} & r_{23} & t_y \\ r_{31} & r_{32} & r_{33} & t_z \\ 0 & 0 & 0 & 1 \end{bmatrix} \tag{11}$$

Among them, r11-r33 are the elements of rotation matrix, and should obey the orthogonality and normality conditions. t_x, t_y and t_z are the translation elements. The indices vector P_{us} with the scalars is

$$V = \begin{bmatrix} s_x \cdot u \\ s_y \cdot v \\ s_z \cdot 0 \\ 1 \end{bmatrix} \tag{12}$$

s_x and s_y are the scale factors and are changed according to the depth and some other parameters from ultrasound device. After the matrix and the vector are multiplied together, we get

$$T \cdot V = \begin{bmatrix} r_{11} & r_{12} & r_{13} & t_x \\ r_{21} & r_{22} & r_{23} & t_y \\ r_{31} & r_{32} & r_{33} & t_z \\ 0 & 0 & 0 & 1 \end{bmatrix} \cdot \begin{bmatrix} s_x \cdot u \\ s_y \cdot v \\ s_z \cdot 0 \\ 1 \end{bmatrix} = \begin{bmatrix} r_{11} \cdot s_x & r_{12} \cdot s_y & r_{13} \cdot s_z & t_x \\ r_{21} \cdot s_x & r_{22} \cdot s_y & r_{23} \cdot s_z & t_y \\ r_{31} \cdot s_x & r_{32} \cdot s_y & r_{33} \cdot s_z & t_z \\ 0 & 0 & 0 & 1 \end{bmatrix} \cdot \begin{bmatrix} u \\ v \\ 0 \\ 1 \end{bmatrix} \quad (13)$$

The SVD method we used in the calibration is to calculate the final matrix:

$$T_c = \begin{bmatrix} r_{11} \cdot s_x & r_{12} \cdot s_y & r_{13} \cdot s_z & t_x \\ r_{21} \cdot s_x & r_{22} \cdot s_y & r_{23} \cdot s_z & t_y \\ r_{31} \cdot s_x & r_{32} \cdot s_y & r_{33} \cdot s_z & t_z \\ 0 & 0 & 0 & 1 \end{bmatrix} \quad (14)$$

At this time, only the first two columns scalar s_x and s_y are compared for the third column is not meaningful for the 2D ultrasound probe. The orthogonality should be 0.0 in the idea condition.

3. RESULTS

In the experiment, we recorded all the data for three different group positions. For each group, nine different indices of the needle tip and the tracking information were recorded as the input. In each group, three to nine frames were used to compute the calibration matrix using the previously discussed equations. Two groups served as target point sets for validating the generated matrix. The results are shown in Table 1. Although the minimum requirement to calculate the calibration matrix is three frames, six or more frames provide increased accuracy. In these data, the maximum RMS calibration error is 1.22mm and the maximum target validation error is 3.45mm. Considering that we used the electromagnetic tracking system, which is not as accurate as an optical tracking system, our proposed method seems reasonably accurate. For each group, the first row is the RMS calibration error with different frame number, and the following two rows are the respective RMS target validation error. The bold value is the maximum error using six or more points for calibration.

Calibration Group	Validation Group	Number of points						
		3	4	5	6	7	8	9
1		0.00	0.47	0.55	0.60	0.70	**1.22**	1.19
1	2	3.13	2.35	2.40	2.42	1.74	1.58	1.78
1	3	3.28	2.63	2.81	2.79	2.43	3.21	**3.45**
2		0.00	0.48	0.59	0.60	0.57	0.66	0.76
2	1	4.77	4.55	3.07	2.50	2.62	2.45	2.20
2	3	5.95	4.63	1.74	2.09	2.01	1.73	2.06
3		0.00	0.42	0.49	0.46	0.44	0.45	0.44
3	1	15.43	3.04	3.22	3.28	3.33	3.16	3.21
3	2	8.31	2.47	2.34	2.37	2.32	2.32	2.32

Table 1 Calibration and validation result (mm)

The validation method we proposed is also verified by three different groups. For each group, the orthogonality and the s_x and s_y are calculated respectively. The orthogonality should be close to 0.0 and the s_x and s_y should remain constant under ideal conditions. Through the validation result, as shown in Table 2, our calibration method gives a reasonable output and is considered to fit those orthogonality and scale conditions. When the frame number is increased to more than six, the orthogonality is close to 0.0 and the scale of the X and Y axis are consistent.

(a) Group 1

Frame	Orthogonality	Scale X	Scale Y
3	0.0415	0.160	0.156
4	0.0545	0.158	0.156
5	0.0620	0.158	0.155
6	0.0526	0.158	0.157
7	0.0264	0.155	0.157
8	0.00219	0.153	0.158
9	-0.0144	0.152	0.157

(b) Group 2

Frame	Orthogonality	Scale X	Scale Y
3	-0.252	0.147	0.173
4	-0.214	0.151	0.169
5	-0.00885	0.152	0.170
6	0.0108	0.153	0.161
7	-0.00232	0.153	0.157
8	-0.00245	0.153	0.157
9	-0.00249	0.153	0.156

(c) Group 3

Frame	Orthogonality	Scale X	Scale Y
3	-0.504	0.156	0.131
4	-0.0439	0.156	0.161
5	-0.0258	0.155	0.157
6	-0.0360	0.155	0.157
7	-0.0326	0.155	0.156
8	-0.0225	0.156	0.157
9	-0.0201	0.156	0.156

Table 2 Validation of orthogonality and scale of calibration matrix

After the calibration, the output matrix is used in our image-guided surgical system, Navigator, to display the freehand ultrasound image plan. The reconstructed 2D beam plane is displayed in 3D to show the correct relationship with the volume-rendered image. The reconstructed CT image can also be displayed simultaneously to compare the difference between the two imaging modalities, providing more information for the planned intervention. The results from the phantom study are shown in Figure 4. Several skin fiducials and one tracked needle are used for registration. After calibration and registration, the related ultrasound image and reformatted CT image are displayed together, in which the simulated aorta is identified. The co-registered images from a swine study are also shown in Figure 5. The swine study was part of an approved protocol. As a part of the open source project titled Image Guided Surgical Toolkit (IGSTK), the source code of the pivot calibration and point-based calibration parts can be downloaded from www.igstk.org.

4. CONCLUSIONS AND DISCUSSIONS

We have performed ultrasound calibration using the tip of an electromagnetically tracked needle as the calibration device, rather than a phantom. A new mathematical linear algebra matrix operation was derived to solve the calibration matrix. The validation method of our algorithm is also included. The results of our experiments prove that this is a feasible calibration method for tracking-based surgical navigation systems.

There are a number of requirements for proper implementation of our point-based calibration method. First, a tracked sensor must be attached to the ultrasound probe, which is necessary for image-guided procedures. Second, a good image, in which the tip of the tracked needle is easily identified, is also required. This can be seen from the acquired image shown in Figure 2. If we fix the ultrasound probe in a stable position and move the tracked needle, the exact position of where the needle tip is passing by the beam plane can be easily identified by image subtraction. The

tracker information with the same time stamp will be recorded and set as the input as well as the pointer coordinate. This will greatly accelerate the calibration speed and requires only minutes for accurate calibration.

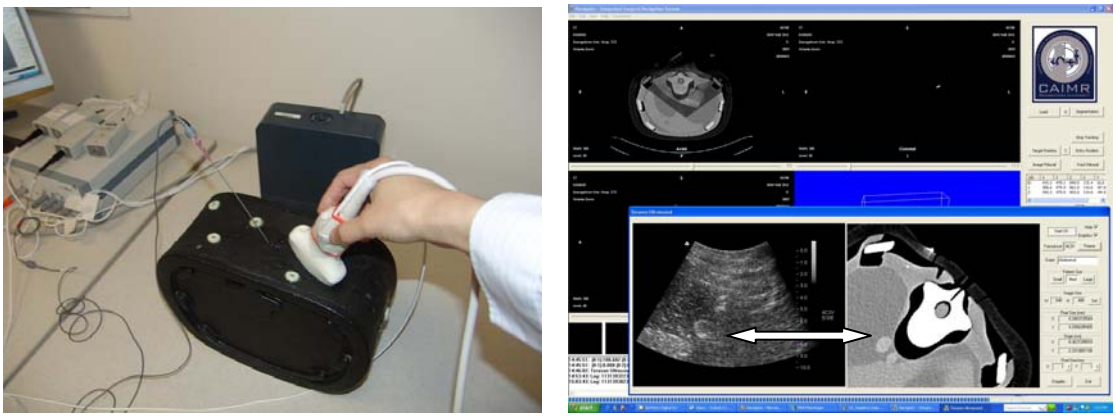

Figure 4: Phantom setup and the US-CT image display in Navigator system

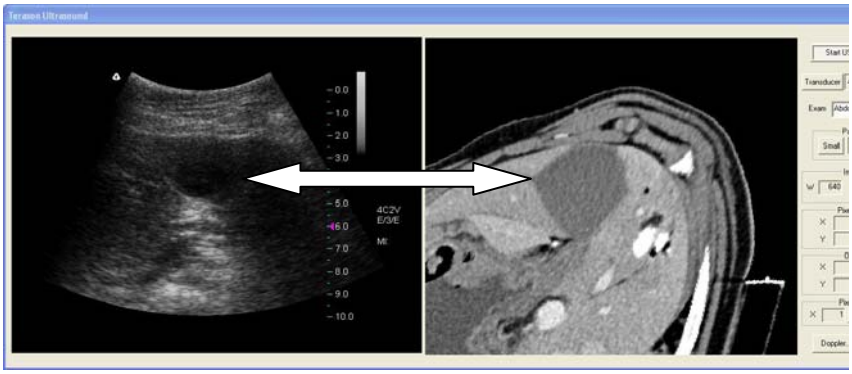

Figure 5: Corresponding US and CT images from swine study showing the swine gallbladder

ACKNOWLEDGEMENTS

This work was funded by US Army grant DAMD17-99-1-9022 and W81XWH-04-1-0078. We would like to thank Northern Digital Inc. for their technical assistance and product support with the AURORA system.

REFERENCES

1. R. W. Prager, R. N. Rouhling, A. H. Gee, and L. Berman, "Rapid calibration for 3-D freehand ultrasound", *Ultrasound in Med. & Biol*., Vol. 24, No. 6, pp. 855-869 (1998)
2. Pagoulatos N, Haynor DR, Kim Y., "A fast calibration method for 3-D tracking of ultrasound images using a spatial localizer", *Ultrasound Med Biol.* Vol. 27, No. 9, pp. 1219-1229 (2001)
3. Nicolas Andreff, Radu Horand, Bernard Espiau, "Robot Hand-Eye Calibration Using Structure-from-Motion", *The International Journal of Robotics Research*, Vol. 20, No. 3, pp. 228-248 (2001)
4. A. Viswanathan, E.M. Boctor, R.H.Taylor, G.D. Hager and G. Fichtinger, "Immediate ultrasound calibration with three poses and minimal image processing", *MICCAI 2004, Saint-Malo, France*. Vol. 3217, pp. 446-454 (2004)
5. Boctor, Emad M.; Jain, Ameet; Choti, Michael A.; Taylor, Russell H.; Fichtinger, Gabor, "Rapid calibration method for registration and 3D tracking of ultrasound images using spatial localizer", *Medical Imaging 2003: Ultrasonic Imaging and Signal Processing. Edited by Walker, William F.; Insana, Michael F. Proceedings of the SPIE*, Vol. 5035, pp. 521-532 (2003)

6. Sebastian Eulenstein and Thomas Lange and M. Hünerbein and Peter Schlag and Hans Lamecker, “Ultrasound Based Navigation System Incorporating Preoperative Planning for Liver Surgery”, *Proceeding of Computer Assisted Radiology and Surgery*, vol. 1268, pp. 758-763 (2004)
7. Lionel G Bouchet, Sanford L Meeks, Gordon Goodchild, Francis J Bova, John M Buatti, and William A Friedman, “Calibration of three-dimensional ultrasound images for image-guided radiation therapy”, *Phys. Med. Biol*. Vol. 46, pp. 559-577 (2001)
8. Aaron Fenster, Donal B Downey, and H Neale Cardinal, “Three-dimensional ultrasound imaging”, *Phys. Med. Biol.* Vol. 46, pp.67-99 (2001)
9. Laurence Mercier, Thomas Lango, Frank Lindseth, D. Louis Collins, “A review of calibration techniques for freehand 3-D ultrasound systems”, *Ultrasound in Med. & Biol.*, Vol. 31, No. 4, pp. 449-471 (2005)
10. Blackall JM, Rueckert D, Maurer CR, er al. “An image registration approach to automated calibration for freehand 3D ultrasound”. *Proceedings of Medical Image Computing and Computer-Assisted Intervention (MICCAI) 2000*, Vol. 1935, pp. 462-471 (2000)
11. Leotta DF, Detmer PR, Martin RW. “Performance of a miniature magnetic position sensor for three-dimensional ultrasound imaging”. *Ultrasound in Med. & Biol.*, Vol. 23, No. 4, pp. 597-609 (1997)
12. Diane M. Muratore, Robert L. Galloway, “Beam calibration without a phantom for creating a 3-D freehand ultrasound system”, *Ultrasound in Med. & Biol.*, Vol. 27, No. 11, pp. 1557-1566 (2001)
13. Kevin Cleary, Hui Zhang, Neil Glossop, Elliot Levy, Filip Bonavac, “Electromagnetic Tracking for Image-Guided Abdominal Procedures: Overall System and Technical Issues”, *IEEE EMBC 2005, Shanghai, China, Sep 1-4*, pp. 268 (2005)
14. Berthold K. P. Horn, “Closed-form Solution of Absolute Orientation using Unit Quaternions”, *Journal of the Optical Society of America A*, Vol. 4, pp. 629-642 (1987)